Astrochemistry VII – Through the Cosmos from Galaxies to Planets
Proceedings IAU Symposium No. 332, 2017
M. Cunningham, T. Millar & Y. Aikawa, eds.

doi:10.1017/S1743921317011589

The Remarkable Molecular Content of Planetary Nebulae

D. R. Schmidt[1] **and L. M. Ziurys**[1,2]

[1]Department of Astronomy, University of Arizona,
933 North Cherry Avenue, Tucson, AZ 85719
email: drschmidt@email.arizona.edu

[2]Department of Chemistry and Biochemistry, University of Arizona
1306 E. University Blvd., Room 221, Tucson, AZ 85721
email: lziurys@email.arizona.edu

Abstract. In order to further define the molecular content of planetary nebulae (PNe), we have conducted searches for HCN, HCO^+, HNC, and CCH at millimeter wavelengths in a sample of seventeen PNe using the new 12 m and Sub-Millimeter Telescopes of the Arizona Radio Observatory (ARO). HCN and HCO^+ were identified in 75 % of the PNe, with corresponding fractional abundances of $f(HCN/H_2) \sim 0.1\text{-}9.1 \times 10^{-7}$ and $f(HCO^+/H_2) \sim 0.04\text{-}7.4 \times 10^{-7}$. HNC was subsequently identified in twelve PNe with $f(HNC/H_2) \sim 0.02\text{-}2.2 \times 10^{-7}$. The [HCN]/[HNC] ratio was found to be ∼1-8 in nebulae observed. CCH was also detected in eight PNe. The abundances for all molecules were found to remain relatively constant with nebular age across 10,000 years, in contrast to model predictions. They are also 10-100 greater than those observed in diffuse clouds, and suggest that molecular material from PNe seed the diffuse ISM.

Keywords. ISM: molecules - planetary nebulae: general - radio lines: ISM

Planetary nebulae (PNe) represent the final stage of evolution for low- to intermediate-mass stars ($M_* \sim 0.5\text{-}8\ M_{sol}$), which make up the majority of stars in the Galaxy. During the asymptotic giant branch (AGB) phase, such stars lose copious amounts of atomic and molecular material (upwards of $10^{-4}\ M_{sol} yr^{-1}$) in the form of a superwind, from which a circumstellar envelope arises (e.g., Kwok 2000). The remnant stellar core, evolving toward a white dwarf, continues to increase in temperature until, at a temperature of 30,000 K, it is capable of ionizing the remnant material in the surrounding shell, thereby creating a PN. The powerful ultraviolet radiation field from this central white dwarf (10^5 times that of the interstellar medium, or ISM) is expected to photodissociate any remnant molecular content in the PN envelope within ∼1000 years (e.g., Redman *et al.* 2003).

In spite of this, the presence of molecular material in PNe has been found to be a common occurrence, rather than the exception. Since the 1970s, CO and H_2 have been detected in numerous PNe, particularly through large-scale surveys (e.g., Huggins & Healy 1989; Huggins *et al.* 1996, 2005; Hora *et al.* 1999; Likkel *et al.* 2006). Further, targeted searches in a number of PNe have revealed a diverse array of polyatomic molecules. The Helix Nebula, for instance, one of the oldest and most well-studied PNe, has been identified in transitions of HCO^+, HCN, HNC, CCH, $c\text{-}C_3H_2$, and H_2CO (Bachiller *et al.* 1997; Tenenbaum *et al.* 2009). Subsequent mapping studies have shown that this molecular material is located throughout the PN (Zeigler *et al.* 2013; Zack and Ziurys 2013). The young PNe NGC 7027 and NGC 6537 have been detected in transitions of HCN, HNC, CCH, CS, SO, H_2CO, HCO^+, and N_2H^+ (Zhang *et al.* 2008; Edwards and Ziurys 2013), while the molecules SiO, SO, and SO_2 have been identified toward the middle-age

PN M2-48 (Edwards and Ziurys 2014). Remarkably enough, a molecule as complex as C_{60} has been observed in a handful of PNe (Cami *et al.* 2010; García-Hernández *et al.* 2010, 2011, 2012; Otsuka *et al.* 2013). Indeed, PNe have been found to be a veritable goldmine of polyatomic molecules; as the Helix proves, even the oldest nebulae can harbor significant quantities of molecular material. The survival of such material long past its expected destruction is thought to be due to shielding provided by high-density clumps of gas and dust. Such clumps, known as cometary globules, have been observed in a handful of PNe, such as NGC 6302 (Santander-García *et al.* 2017), NGC 7293, and NGC 6853 (O′Dell and Handron 1996; O′Dell *et al.* 2002).

Aside from a handful of targeted searches, however, most PNe have not had their molecular content explored in any detail beyond CO and H_2, if at all. Given that most stars will pass through the PN stage at the end of their lives, it is vital to understand the molecular composition of these nebulae, how it evolves over the course of the PN stage, and what role PNe play in seeding the ISM. In order to elucidate the answers to these questions, we undertook a search for a range of polyatomic molecules in a set of PNe which had previously been detected in CO. This work began in 2012, with a search for HCN and HCO^+ in seventeen nebulae (Schmidt and Ziurys 2016). HCN and HCO^+ were chosen due to their high dipole moments (2.98 D and 3.9 D, respectively), which allow them to be used as dense-gas tracers, and their chemical significance (HCO^+ is a tracer of ion-molecule chemistry, while HCN can be compared to its isomer HNC). The seventeen target PNe were selected from the CO surveys of Huggins and Healy (1989), Huggins *et al.* (1996), and Huggins *et al.* (2005). All sources had a measured CO J=2→1 line temperature of at least 50 mK and did not have any previously known HCN or HCO^+ emission. Notably, these PNe span a range of ages, sizes, and morphologies, including young, small sources such as K3-17 and K3-45 and large, old nebulae like NGC 6772. As a result, molecular abundances could be examined with respect to such factors.

Rotational transitions of HCN and HCO^+ were searched for in these seventeen objects using the facilities of the Arizona Radio Observatory (ARO). The 3 mm, dual polarization receiver of the ARO 12 m Telescope at Kitt Peak (both the original as well as the recently installed former European ALMA prototype antenna) was used to observe the J=1→0 line of both molecules; to study the J=3→2 transitions, the 1.3 mm dual polarization receiver of the ARO Submillimeter Telescope (SMT) on Mt. Graham, Arizona was employed (see Schmidt and Ziurys (2016) for observational details). Of the seventeen PNe, eleven were detected in at least one transition of HCN, and ten in one transition of HCO^+ (with one nebula, K4-47, having been detected in HCO^+ prior to this survey by Edwards *et al.* (2014)). The HCN spectra for K4-47, in addition to those for many other molecules observed in this source, are given in Figure 1. Further, details on the sources detected in HCN and/or HCO^+ are provided in Table 1.

HCN and HCO^+ column densities were estimated from these data using the non-LTE radiative transfer code, RADEX. For details of this analysis, see Schmidt and Ziurys (2016). The resulting column densities varied from N_{tot}(HCN) $\sim$ 0.2-27 $\times$ 10^{13} cm-2 and $N_{tot}(HCO^+)$ $\sim$ 0.3-8.7 $\times$ 10^{13} cm^{-2}. Corresponding abundances with respect to H_2 were calculated, resulting in ranges of $f(HCN/H_2)$ $\sim$ 0.1-9.1 $\times$ 10^{-7} and $f(HCO^+/H_2)$ $\sim$ 0.04-7.4 $\times$ 10^{-7}.

In addition to reinforcing the idea that polyatomic molecules are common constituents of PNe, one remarkable outcome of this work is the apparent lack of evolution of molecular abundance over the nebular lifetime. Figure 2 demonstrates this conclusion with a plot of abundance versus age for the planetary nebulae observed, with circles representing the sources observed by Schmidt & Ziurys (2016; 2017a,b) and stars representing those previously measured. Here, red represents HCN while blue represents HCO^+. Also plotted

Table 1. Summary of Observed Planetary Nebulae

Source	Age[a] (years)	Morphology / C/O [a]	Molecules Detected by Schmidt and Ziurys (2016, 2017a,b)
Hb 5	1500	bipolar, C-rich	HCN, HCO^+, HNC, CCH
K3-17	970	bipolar	HCN, HCO^+, HNC, CCH
K3-45	830	bipolar	HCN, HNC, CCH
K3-58	11,070	bipolar	HCN, HCO^+, HNC, CCH
K3-83	4600	bipolar	HCO^+
M1-7	6000	bipolar, C/O=1.1	HCN, HCO^+, HNC, CCH
M2-9	2500	bipolar, C/O<0.5	HCO^+
M3-28	7700	quadrupolar	HCN, HCO^+, HNC, CCH
M3-55	5040	bipolar	HCN, HCO^+, HNC, CCH
M4-14	5550	quadrupolar	HCN, HCO^+, HNC, CCH
NGC 2440	3400	quadrupolar (?), C/O=1.1-1.9	HCN, HCO^+, HNC
NGC 6772	10,900	elliptical	HCN, HNC
K4-47	900	bipolar, C-rich (?)	HCN, HNC, CCH
NGC 7293	12,000	bipolar	HCN, HNC

[a] See Schmidt and Ziurys (2016, 2017a,b) for reference information.

are the predictions of Redman *et al.* (2003) (using triangles), whose model considered the evolution of a wide array of molecules in the envelopes of PNe up to an age of 10,050 years. As the plot demonstrates, while the model of Redman *et al.* (2003) predicts significant destruction of HCN between 2550 and 10,000 years and consistently low abundances of HCO^+ (between 10^{-10} and 10^{-12}), our measured abundances show little temporal variation and abundances that are much higher than those predicted by the model at all stages. Further, the PN abundances are seen to be on the order of 1-2 magnitudes greater than those reported for diffuse clouds (e.g., Liszt *et al.* 2006). This is consistent with the idea that dense globules harboring molecules in PNe disperse into the diffuse ISM and seed it with molecular material.

Upon completion of this survey, we commenced a search for HNC in the eleven PNe in which HCN had been identified, with the goal of measuring [HCN]/[HNC] ratios. While HCN and HNC are both predicted to be produced through dissociative recombination of HCNH+ in equal amounts, the ratio in AGB stars is skewed far from unity due to the hot, LTE chemistry in the inner envelope, which favors HCN. The ratio was though to decrease from the AGB stage through the protoplanetary nebula (PPN) and PN stages; however, few PNe had been detected in transitions of both molecules, and accurate measures of the [HCN]/[HNC] ratio were difficult to come by. The $J = 1 \rightarrow 0$ and $J = 3 \rightarrow 2$ transitions of HNC were measured, once again with the new ARO 12 m and Submillimeter Telescopes (see Schmidt and Ziurys (2017a)). In addition, eight positions of the Helix Nebula, which had previously been detected in H_2CO, HCO^+, and CO by Zack & Ziurys (2013), were also observed at the $J=1 \rightarrow 0$ transition frequencies of HCN and HNC in order to analyze the ratio across the nebula.

HNC was detected in at least one transition in all the nebulae studied, and HCN and HNC were identified at all positions observed in the Helix. The HNC spectra obtained for K4-47 are displayed in Figure 1, while the HCN and HNC spectra for all positions of the Helix are shown in Figure 3. Once again, column densities were determined using RADEX in a similar fashion as that described for HCN and HCO^+; for details, see Schmidt & Ziurys (2017a). For the Schmidt & Ziurys (2016) survey sources, the HNC column densities were found to range from $\sim(0.06\text{-}4.0) \times 10^{13}$ cm^{-2}. Helix column densities ranged from $\sim(0.2\text{-}2.4) \times 10^{12}$ cm^{-2} for HCN and $(0.07\text{-}1.6) \times 10^{12}$ cm^{-2} for HNC. Once again, fractional abundances were calculated with respect to H_2, and were found to range

https://doi.org/10.1017/S1743921317011589 Published online by Cambridge University Press

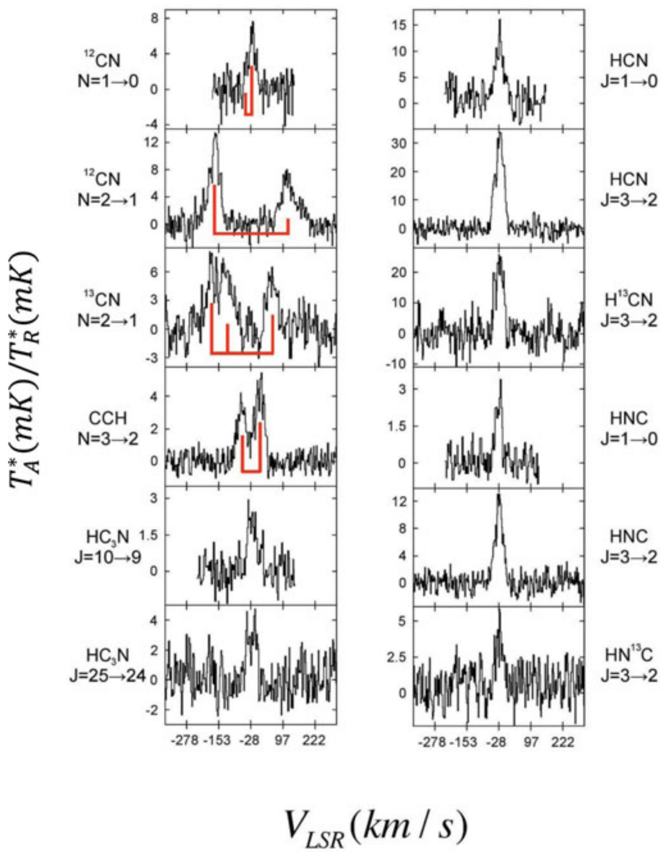

Figure 1. Spectra of the molecular transitions observed toward the planetary nebula K4-47 using the 12 m and Submillimeter Telescopes of the Arizona Radio Observatory. These include the ^{12}CN N=1→0 and N=2→1 transitions at 113 and 226 GHz, ^{13}CN: N=2→1 line at 217 GHz, CCH: N=3→2 line at 262 GHz, HC_3N: J=10→9 and J=25→24 transitions at 91 and 227 GHz, HCN: J=1→0 and J=3→2 lines at 88 GHz and 265 GHz, $H^{13}CN$: J=3→2 line at 259 GHz, HNC: J=1→0 and J=3→2 lines at 90 GHz and 271 GHz, $HN^{13}C$: J=3→2 line at 261 GHz. The strongest components of the CN hyperfine and CCH spin-rotation structures are indicated under the respective spectra.

from $f(\mathrm{HNC/H_2}) \sim (0.02\text{-}1.4) \times 10^{-7}$ for the survey sources. The fractional abundances for the Helix were found to be $f(\mathrm{HCN/H_2}) \sim (0.2\text{-}3.2) \times 10^{-7}$ and $f(\mathrm{HNC/H_2}) \sim (0.09\text{-}2.2) \times 10^{-7}$. The resulting [HCN]/[HNC] ratios were determined to vary between 2-8 for the survey sources and from 1-4 for the Helix.

The HNC abundances measured in this work showed no temporal variation, as opposed to the predictions of Redman *et al.* (2003) (see Figure 2; cyan symbols represent HNC measurements/expectations). While the model of Redman *et al.* (2003) predicted a sharp decrease of 10^4 by 6000 years, with a steady abundance of 10^{-12} thereafter, abundances calculated for our sources fell into the range $\sim 10^{-8} - 10^{-7}$, with no significant change between 1000 to 11,000 years. Further, the [HCN]/[HNC] ratios established in this work are notably constant with nebular age. These ratios are comparable to those measured for PPNe, and are significantly lower than those found for AGB stars (Woods *et al.* (2003), for instance, measured ratios of 40-300 for seven carbon stars). It is thought that the ratio significantly decreases in the PPN stage due to the increase in ionization, which drives reactions leading to the formation of $HCNH^+$, an intermediate in the formation of HNC

https://doi.org/10.1017/S1743921317011589 Published online by Cambridge University Press

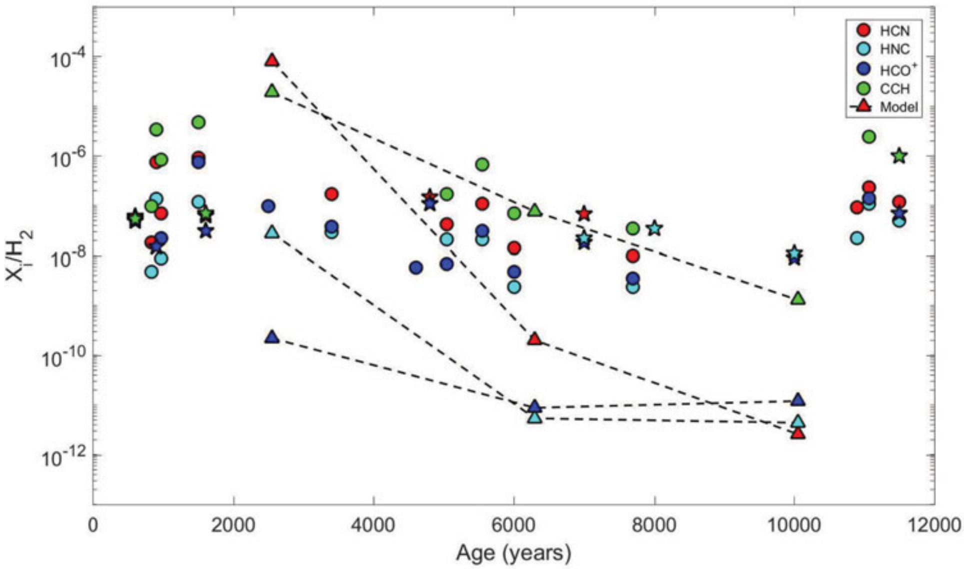

Figure 2. A plot of fractional abundances of HCN (red), HCO^+ (blue), HNC (cyan), and CCH (green) relative to H_2 in PNe vs. the ages of the PNe (in years). Circles represent data from the work of Schmidt and Ziurys (2016, 2017a,b), while stars indicate measurements for NGC 7027, NGC 6537, M2-48, NGC 7293, NGC 6853, M4-9, NGC 6781 and NGC 6720 from previous studies (see Schmidt and Ziurys 2016, 2017a; Zhang *et al.* 2008; Edwards and Ziurys 2013; Tenenbaum *et al.* 2009; Bachiller *et al.* 1997). The red, blue, cyan, and green triangles (with dashed lines) designate the fractional abundances for HCN, HCO^+, HNC, and CCH, respectively, from the model of Redman *et al.* (2003). The measured abundances of all molecules appear to stay relatively constant across the 10,000-year lifetime of PNe, while the model predicts a significant decrease during this time period.

through dissociative recombination. These and other reactions modify the [HCN]/[HNC] ratio, bringing it closer to unity with time. Based on our observations in PNe, we suggest that the chemistry which adjusts the abundances of AGB stars occurs primarily in the PPN stage, allowing the [HCN]/[HNC] ratio to freeze out in the PN phase. The fact that the ratio is remarkably consistent across the Helix Nebula provides further proof for the freeze-out hypothesis.

Additionally, comparison of the measurements presented in Schmidt and Ziurys (2017a) with those made in diffuse clouds by Liszt & Lucas (2001) and Liszt *et al.* (2006) once again show that the abundances measured in PNe are on the order of 1-2 orders of magnitude higher than those in diffuse clouds. Further, the average [HCN]/[HNC] ratio of 5 measured in diffuse clouds is comparable to those determined for PNe. This result is additional evidence that PNe seed the diffuse ISM with molecular material protected in dense clumps of gas and dust, which subsequently disperse into the surrounding medium. The gas is too diffuse for significant chemistry such that the [HCN]/[HNC] ratio remains fairly constant.

It is interesting that the ^{13}C isotopologues of HCN, HNC, and CN were often observed in these sources, when actually searched for. The carbon-13 species was observed in all three species in K4-47, for example, as shown in Figure 1. These three species suggest a $^{12}C/^{13}C$ ratio of $\sim$ 2-3. Considering the carbon-rich nature of this object, this very low ratio suggests that a J-type star was the progenitor for K4-47.

Due to the likelihood that the PNe containing both HCN and HNC are carbon-rich sources, we decided to initiate a search for CCH in the eleven PNe in which both molecules

https://doi.org/10.1017/S1743921317011589 Published online by Cambridge University Press

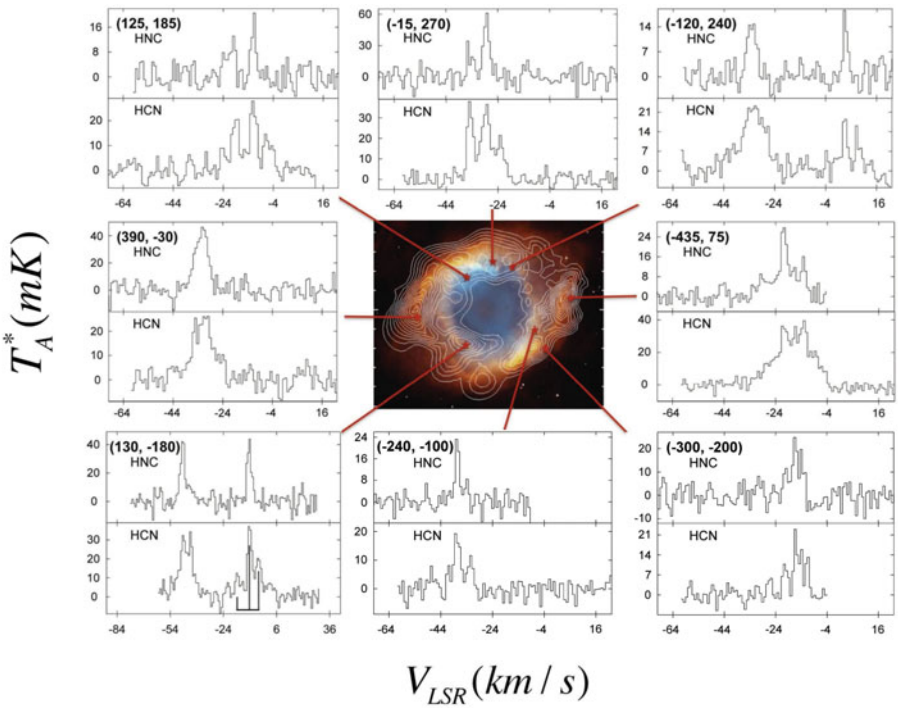

Figure 3. Spectra of the J = 1→0 transitions of HNC (upper panel) and HCN (lower panel) observed toward eight positions in the Helix Nebula, using the ARO 12 m telescope, the ALMA European prototype antenna. The R.A. and decl. offsets for each position (in arcseconds from the central star) are displayed in the top left corner of each panel. The HCN LTE hyperfine pattern is shown beneath the 10 km s^{1} velocity component of the (130, 180) spectrum. Positions are indicated on an optical image of the Helix (NASA *et al.* 2003). Overlaid contours on the image indicate the peak brightness temperature of the J = 1→0 transition of HCO^+ (from Zeigler *et al.* 2013). HCN and HNC are clearly visible in all positions, showing that these molecules have a widespread distribution in the nebula, and trace the complex, bipolar velocity structure of this object seen in HCO^+.

had been detected. Furthermore, two PNe in which C_{60} had previously been identified (M1-12 and M1-20; García-Hernández *et al.* 2010) were also observed. These targets were selected as C_2 is seen to be a building block of C_{60} in the laboratory, as well as a by-product of fragmentation of large carbon clusters. Given the inability for C_2 to be detected in the millimeter regime due to its lack of an electric dipole moment, CCH is a proxy, thereby allowing the exploration of the potential connection between C_{60} and C_2 in space. The results of this search will be published in a forthcoming work (Schmidt and Ziurys 2017b).

Using the facilities of the ARO, the N=1→0 and N=3→2 transitions of CCH were observed toward these target sources. Of the thirteen target sources, nine were detected in at least one transition of CCH, all from the original Schmidt and Ziurys surveys. Through a similar analysis to those for HCN, HCO^+, and HNC, column densities were determined, and were seen to range between 0.2-3.3 $\times$ 10^{15} cm^{-2}. Correspondingly, fractional abundances varied between $\sim$0.02-4.7 $\times$ 10^{-6}. One of the primary outcomes of this work was, once more, the lack of variation in abundance with nebular age (see Figure 2; green symbols represent CCH measurements/predictions). Redman *et al.* (2003) expect a decline in abundance of 10^4 over the course of the nebular lifetime; however, our measurements show that the ratio remains within the range of $\sim 10^{-7}$-10^{-6} over this time. Further, these abundances are approximately 1-2 orders of magnitude greater than those measured in diffuse clouds (Lucas & Liszt 2000; Gerin *et al.* 2011), adding yet more evidence to the seeding hypothesis described earlier.

Overall, the main conclusions from each of the surveys described above can be summarized as follows: (1) polyatomic molecules are a common constituent of PNe regardless of age, size, and morphology, (2) abundances of all molecules studied show no variation with nebular age, in contrast to the predictions of chemical models, (3) abundances of all molecules compared with those measured for diffuse clouds are consistent with the idea that dense clumps of gas and dust in PNe disperse into the surrounding ISM, thereby seeding it with molecular material. More observations of a greater number of PNe and a wider variety of molecules will of course be necessary in order to provide a fuller understanding of the molecular content of PNe. However, observations of PNe like K4-47 (see Figure 1) already prove that such an undertaking can be incredibly fruitful.

References

Bachiller, R., Forveille, T., Huggins, P. J., & Cox, P. 1997, *A&A*, 324, 1123
Cami, J., Bernard-Salas, J., Peeters, E., & Malek, S. E. 2010, *Sci*, 329, 1180
Edwards, J. L. & Ziurys, L. M. 2013, *ApJL*, 770, L5
Edwards, J. L., Cox, E. G., & Ziurys, L. M. 2014, *ApJ*, 791, 79
Edwards, J. L. & Ziurys, L. M. 2014, *ApJL*, 794, L27
García-Hernández, D. A., Iglesias-Groth, S., & Acosta-Pulido, J. A., *et al.* 2011, *ApJL*, 737, L30
García-Hernández, D. A., Manchado, A., & Garca-Lario, P., *et al.* 2010, *ApJL*, 724, L39
García-Hernández, D. A., Villaver, E., & Garca-Lario, P., *et al.* 2012, *ApJ*, 760, 107
Gerin, M., Kamierczak, M., Jastrzebska, M., *et al.* 2011, *A&A*, 525, A116
Hora, J. L, Latter, W. B., & Deutsch, L. K. 1999, *ApJS*, 124, 195
Huggins, P. J., Bachiller, R., Cox, P., & Forveille, T. 1996, *A&A*, 315, 284
Huggins, P. J., Bachiller, R., Planesas, P., Forveille, T., & Cox, P. 2005, *ApJS*, 160, 272
Huggins, P. J. & Healy, A. P. 1989, *ApJ*, 346, 201
Kwok, S. 2000, The Origin and Evolution of Planetary Nebulae (Cambridge: Cambridge Univ. Press)
Likkel, L., Dinerstein, H. L., Lester, D. F., Kindt, A., & Bartig, K. 2006, *AJ*, 131, 1515
Liszt, H. & Lucas, R. 2001, *A&A*, 370, 576
Liszt, H. S., Lucas, R., & Pety, J. 2006, *A&A*, 448, 253
Lucas, R. & Liszt, H. S. 2000, *A&A*, 358, 1069
O′Dell, C. R. & Handron, K. D. 1996, *AJ*, 111, 1630
O′Dell, C. R., Balick, B., Hajian, A. R., Henney, W. J., & Burkert, A. 2002, *AJ*, 123, 332
Otsuka, M., Kemper, F., Hyung, S., *et al.* 2013, *ApJ*, 764, 77
Redman, M. P., Viti, S., Cau, P., & Williams, D. A. 2003, *MNRAS*, 345, 1291
Santander-García, M., Bujarrabal, V., Alcolea, J., *et al.* 2017, *A&A*, 597, A27
Schmidt, D. R. & Ziurys, L. M. 2016, *ApJ*, 817, 175
Schmidt, D. R. & Ziurys, L .M. 2017a, *ApJ*, 835, 79
Schmidt, D. R. & Ziurys, L. M. 2017b, submitted
Tenenbaum, E. D., Milam, S. N., Woolf, N. J., & Ziurys, L. M. 2009, *ApJL*, 704, L108
Woods, P. M., Schier, F. L., Nyman, L. Å., & Olofsson, H. 2003, *A&A*, 402, 617
Zack, L. N. & Ziurys, L. M. 2013, *ApJ*, 765, 112
Zeigler, N., Zack, L. N., Woolf, N. J., & Ziurys, L. M. 2013, *ApJ*, 778, 16
Zhang, Y., Kwok, S., & Trung, D.-V. 2008, *ApJ*, 678, 328